Radiation Physics and Chemistry 166 (2020) 108459

Contents lists available at ScienceDirect

Radiation Physics and Chemistry

journal homepage: www.elsevier.com/locate/radphyschem

A simple approach for developing model OF Si(Li) detector in Monte Carlo simulation

Huynh Dinh Chuong[a], Nguyen Thi Truc Linh[a], Le Thi Ngoc Trang[a], Vo Hoang Nguyen[b], Le Hoang Minh[b], Chau Thanh Tai[b], Tran Thien Thanh[a,b,*]

[a] Nuclear Technique Laboratory, University of Science, VNU-HCM, Viet Nam
[b] Department of Nuclear Physics, Faculty of Physics and Engineering Physics, University of Science, VNU-HCM, Viet Nam

ARTICLE INFO

Keywords:
Si(Li) detector
Monte Carlo simulation
MCNP6 code
Efficiency calibration

ABSTRACT

In this paper, a simple approach for developing the model of a Si(Li) detector in Monte Carlo simulations is presented and validated. Experimental measurements using "point-like" standard radioactive sources including ^{133}Ba, ^{137}Cs, ^{152}Eu, ^{154}Eu, ^{241}Am were performed for both configurations with and without collimator, respectively. The MCNP6 code was used for Monte Carlo simulation of photon transport inside the models constructed similar to these configurations. Firstly, an initial model of the Si(Li) detector was constructed based on the manufacturer's specifications, but the simulated efficiency shows a very high discrepancy from the experiment. Then, the critical geometric parameters of the model of Si(Li) detector were improved step-by-step to achieve the optimized model. For the optimized model, a good agreement was obtained between the experimental and simulated results. The relative deviations of experimental and simulated efficiencies are less than 4% with energies in the range of 12–60 keV for both configurations.

1. Introduction

Silicon Lithium (Si(Li)) detectors are widely used both in fundamental researches and in applications to quantitative elemental analysis. In fact, the accurate knowledge of the spectral response and the full energy peak efficiency of the Si(Li) detector is necessary for these purposes. In recent years, the general-purpose Monte Carlo codes (such as GEANT, MCNP) are widely used for simulating the response functions of detectors in radiation measurement. These codes allow users to describe a detailed and complex geometry of the detector and surrounding materials. Therefore, these are convenient and suitable for simulating the response functions of the Si(Li) detectors in different applications. The intrinsic efficiency of the Si(Li) detector in the photon energy range of 2.6–59.5 keV for measurements of radioactive sources and particle-induced X-ray emission (PIXE) was calculated using the Monte Carlo simulation codes MCNP and GEANT4 (Mesradi et al., 2008). The spectral response of the Si(Li) detector for PIXE measurements of mono-elemental samples and complex component samples was calculated using the Monte Carlo simulation code GEANT4 (Francis et al., 2013; Incerti et al., 2015). These simulated results also showed good agreements with experimental data and demonstrated the feasibility of using simulated data into analytical applications.

It is obvious that the information about geometry and properties of the components in experimental set-up (such as detector, source, collimator, shielding layers, etc.) is required for calculating the detector response function by Monte Carlo simulation. The geometric characteristics of detectors are usually provided in the manufacturer's specifications. However, some parameters are not completely presented; for example, information about the gold contact and the dead layer is not shown in the manufacturer's specifications for the Si(Li) detector used in this study. Besides, in general, the nominal value of geometric parameters in the manufacturer's specifications can be significantly different from the real value. There have been several reports about the measured efficiency of Si(Li) detectors which is significantly different from the simulated efficiency on the basis of geometric parameters provided by the manufacturer (Haifa et al., 2007; Mesradi et al., 2008; López-Pino et al., 2013). These results show that the models of Si(Li) detectors constructed by manufacturer's specifications may be invalid. Therefore, the model of the detector should be optimized to reproduce the experimental results from several "point-like" sources before using in Monte Carlo simulation for different applications.

* Corresponding author. Department of Nuclear Physics, Faculty of Physics and Engineering Physics, University of Science, VNU-HCM, 227, Nguyen Van Cu Street, District 5, Ho Chi Minh City, Viet Nam.
E-mail address: ttthanh@hcmus.edu.vn (T.T. Thanh).

https://doi.org/10.1016/j.radphyschem.2019.108459
Received 1 June 2019; Received in revised form 16 August 2019; Accepted 17 August 2019
Available online 19 August 2019
0969-806X/

Table 1
Summarization of the relevant data for radioactive sources used in this study.

Radionuclide	Activity (kBq)	Energy (keV)	Emission intensity (%)
^{133}Ba	27.8 ± 0.8	30.63	33.8
		30.97	62.4
		35.05	18.24
		35.90	4.45
		53.16	2.229
^{137}Cs	33.7 ± 1.0	31.82	1.95
		32.19	3.59
		36.38	1.055
		37.31	0.266
^{154}Eu	24.0 ± 0.7	42.31	7.2
		43.00	13
		48.70	4.1
		50.10	1.08
^{152}Eu	229 ± 7	39.52	20.8
		40.12	37.7
		45.41	11.78
		46.71	3.04
^{241}Am*	34 ± 1	11.87	0.844
		13.95	11.6
		17.75	11.83
		20.82	2.94
		26.34	2.31
		59.54	35.92

Note: ^{241}Am* photon emission intensity using (Lépy et al., 2008), (Chechev and Kuzmenko, 2010), and (Laboratoire National Henri Becquerel, 2019).

Table 2
Parameters of initial model and optimized model for the Si(Li) detector.

Parameters of the Si(Li) detector	Value for initial model	Value for optimized model
Active diameter of crystal (mm)	10.5	9.71
Active thickness of crystal (mm)	5.4	4.8
Groove ID (mm)	11.18	11.18
Groove OD (mm)	15.75	15.75
Groove Depth (mm)	3.56	3.56
Window-crystal distance (mm)	6	8.19
Front dead layer (mm)*	0	0.113
Rear dead layer (mm)*	0	0.486
Gold contact thickness (mm)*	0.0003	0.0003
Beryllium window thickness (mm)	0.125	0.125
Density of silicon (g/cm^3)	2.329	2.329
Density of gold (g/cm^3)	19.29	19.29
Density of stainless steel (g/cm^3)	7.849	7.849
Density of beryllium (g/cm^3)	1.848	1.848
Density of aluminum (g/cm^3)	2.699	2.699
Density of lead (g/cm^3)	11.35	11.35
Density of plastic (g/cm^3)	1.0512	1.0512

Note *: Value of this parameter is not provided by manufacturer.

Many studies have been performed to optimize the model of the detectors for Monte Carlo simulation and can be classified into two different approaches. An approach involves determining the values of the geometric parameters of the surveyed detector by experimental techniques. For example, the precise dimensions and position of Si(Li) crystal inside the cryostat were determined by radiography (Mesradi et al., 2008), computerized tomography (López-Pino et al., 2013) and detector scanning with finely collimated photon beam (Campbell et al., 1984). The optimized models by this approach are close to real geometry of the Si(Li) detector, therefore these are accurate and reliable enough to be used in Monte Carlo simulations for all applications. However, this approach can be difficult to implement for many laboratories, because it requires some specialized equipment. Another approach involves experimentally calibration of the full energy peak efficiency for measurement configurations and then adjustment of the value of some geometric parameters of the detector to reach good agreement between simulated and experimental results (Karamanis,

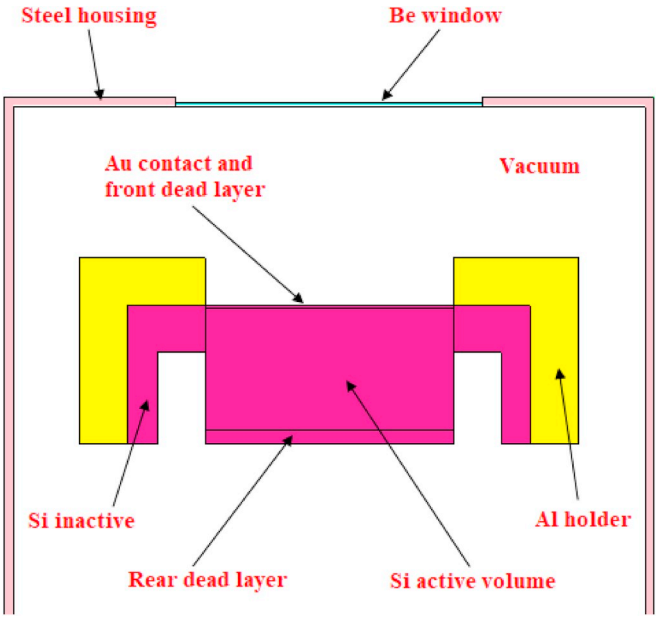

Fig. 1. Schematic representation of the simulated model of Si(Li) detector using MCNP6 code.

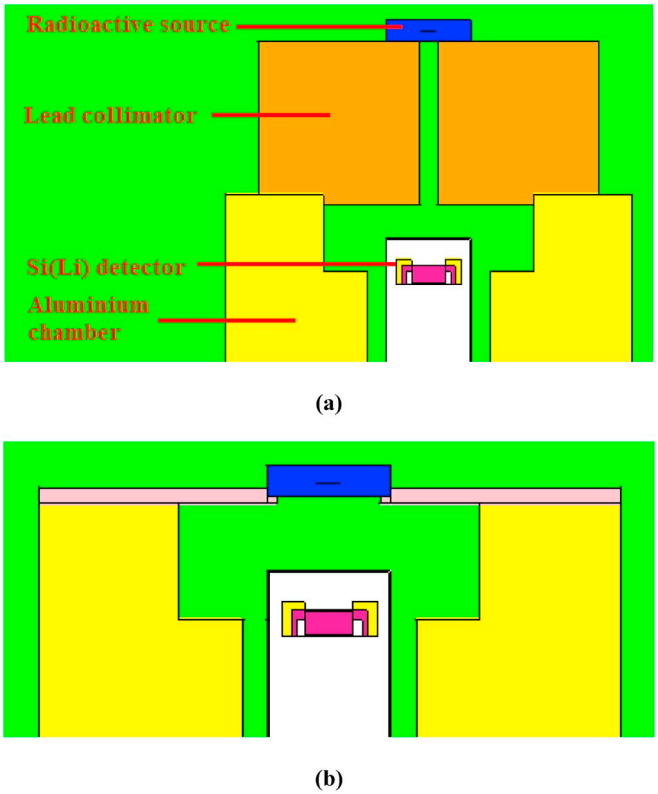

Fig. 2. Schematic representation of the simulated models of the measurement configurations (a) with and (b) without collimator using MCNP6 code.

2003; Haifa et al., 2007). This approach has the advantages to be simple and easy to implement for the laboratories. However, the procedures for optimizing the model of the detector must be carefully considered. Because the full energy peak efficiency depends on various geometric parameters of the detector, the optimization of each parameter may be affected by other parameters. In fact, there is still a lack of reports to describe the detailed procedures based on this approach for optimizing the model of Si(Li) detectors.

Table 3
Comparison between simulated efficiency with the initial model of Si(Li) detector and experimental efficiency for both measurement configurations with and without collimator.

E (keV)	With collimator				Without collimator			
	ε_{exp} ($\times 10^{-4}$)	U_{exp} (%)	ε_{sim} ($\times 10^{-4}$)	RD (%)	ε_{exp} ($\times 10^{-4}$)	U_{exp} (%)	ε_{sim} ($\times 10^{-4}$)	RD (%)
11.87	2.20	3.3	3.76	71	23.38	3.2	54.28	132
13.95	3.26	3.2	4.53	39	34.22	3.2	64.66	89
17.75	4.92	3.2	5.69	16	50.76	3.2	78.99	56
20.82	5.55	3.3	6.15	11	55.80	3.2	82.78	48
26.34	5.65	4.6	5.97	6	52.38	4.6	76.45	46
30.63	4.76	3.2	5.22	10	45.63	3.2	65.05	43
30.97	4.63	3.2	5.15	11.3	44.55	3.2	64.12	44
31.82	4.51	3.6	4.97	10	43.64	3.6	61.66	41
32.19	4.44	3.6	4.89	10	42.68	3.6	60.49	42
35.05	3.86	3.4	4.27	11	35.73	3.4	52.32	46
35.90	3.71	4.0	4.09	10	34.20	4.0	49.95	46
36.38	3.64	3.7	4.00	10	33.64	3.7	48.77	45
37.31	3.45	4.3	3.81	10	32.25	4.3	46.35	44
39.52	3.02	3.3	3.39	12	28.30	3.3	40.98	45
40.12	2.90	3.3	3.29	13	27.94	3.3	39.69	42
42.31	2.63	4.1	2.92	11	23.85	4.1	35.14	47
43.00	2.54	3.8	2.81	11	23.64	3.8	3.73	43
45.41	2.17	3.4	2.47	14	20.29	3.4	29.50	45
46.70	2.04	4.0	2.31	14	19.19	4.0	27.60	44
48.70	1.89	3.9	2.08	10	17.11	3.9	24.68	44
50.10	1.67	4.2	1.94	16	15.52	4.1	22.98	48
53.16	1.45	3.2	1.65	14	13.11	3.2	19.50	49
59.54	1.08	3.0	1.21	12	9.46	3.0	14.18	50

U_{exp} means experimental uncertainty, and RD means relative deviation. $RD(\%) = \frac{|\varepsilon_{sim} - \varepsilon_{exp}|}{\varepsilon_{exp}} \times 100\%$

This paper describes a detailed procedure which is based on the simple approach for optimizing the model of a Si(Li) detector in the Monte Carlo simulation. The procedure only requires experimental measurements using a ^{241}Am "point-like" standard radioactive source for two configurations with and without collimator. The MCNP6 code was used for Monte Carlo simulation of photon transport inside the models constructed similar to these configurations. Firstly, an initial model of the Si(Li) detector was constructed based on the manufacturer's specifications. Then, the critical geometric parameters in the model of Si(Li) detector including the thickness of the front dead layer and rear dead layer, the active diameter of crystal, window-crystal distance were improved step-by-step to achieve the optimized model. For the optimization of each parameter, experimental data (corresponding to different photon energies and configurations) are selected so that their value are only affected by this parameter. The optimized model was validated by comparing the simulations with the experimental data in two configurations.

2. Experimental set-up

2.1. X-ray spectrometer and radioactive sources

A Si(Li) detector (model SL80180) supplied by Mirion Technologies Inc. (Mirion Technologies Inc., 2017a, 2017b) was used in the present study (see Table 2). This detector is connected to a DSA-LX module (Mirion Technologies Inc., 2017a, 2017b) based on advanced digital signal processing techniques, ensuring high-voltage supply, amplification, and shaping of the output pulses. The acquisitions of gamma spectra were driven by Genie-2k version 3.3 software (Genie, 2009). All spectra are recorded using over 16384 channels and energy channel width of 5.68 eV in order to detect photons in the energy range up to 93 keV. The Si(Li) detector is cooled by liquid nitrogen and installed in a room with stable environmental conditions (approximate temperature of 26 °C and humidity of 45%). Under such measurement conditions, it is validated that there was no significant energy shift after checking different spectra.

The standard radioactive sources of type D configuration supplied by Eckert & Ziegler Group (Eckert and Ziegler, 2019), including ^{133}Ba, ^{137}Cs, ^{152}Eu, ^{154}Eu, ^{241}Am with relative combined uncertainties of the reference activities around 3%, were used to provide gamma and X-rays with energies between 12 and 60 keV. These sources are disk-shaped made of high strength plastic with a diameter of 25.4 mm and a thickness of 6.35 mm. The active diameter of the source is 5 mm, and the window thickness is 2.77 mm. Table 1 summarizes the relevant data for these sources.

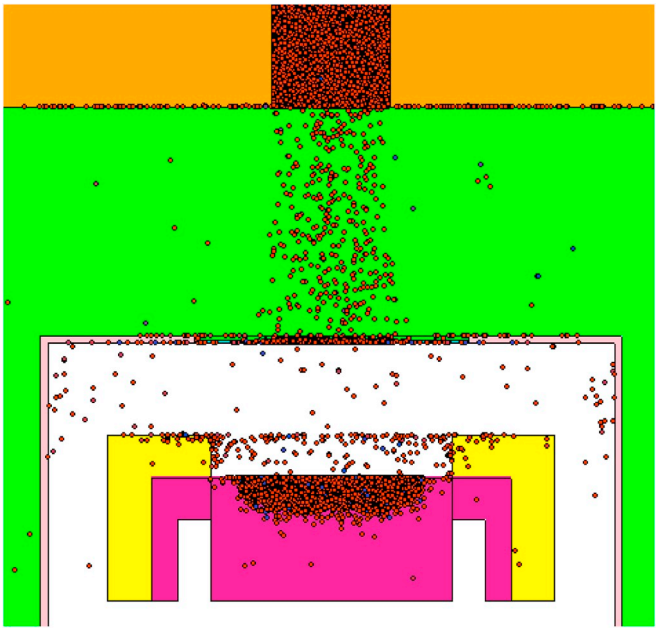

Fig. 3. Tracking of the interactions of photons with energy of 11.87 keV inside the model of Si(Li) detector for measurement configuration with collimator.

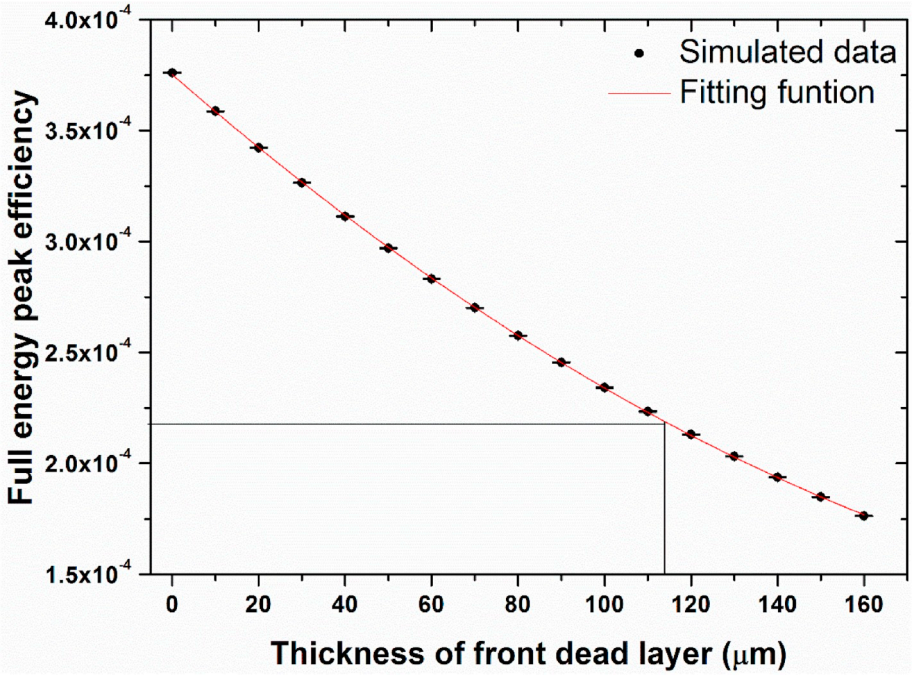

Fig. 4. Fitting with an exponential function of simulated efficiency at energy of 11.87 keV for the measurement configuration with collimator according to the thickness of front dead layer.

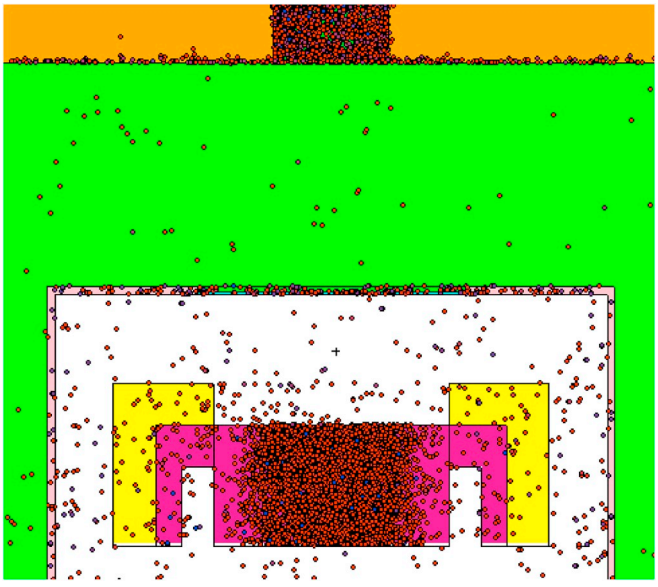

Fig. 5. Tracking of the interactions of photons with energy of 59.54 keV inside the model Si(Li) detector for measurement configuration with collimator.

2.2. Efficiency calibration

In this study, two sets of experiments were performed to determine the absolute efficiency calibration of the Si(Li) detector. Firstly, the "point-like" standard radioactive sources were measured in air on the detector axis at a distance of 15.5 mm from detector's window without collimator. In this experiment, the sources were arranged on a thin plastic support. Secondly, these sources were measured in air on the detector axis at a distance of 58.3 mm from detector's window with a collimator. The collimator is a 48.3 mm thick hollow lead cylinder with 5.65 mm inner diameter and 100 mm outer diameter. The measurements were performed to obtain a number of counts in the interesting peaks ranging from 3×10^4 to 2×10^6. The dead-time was less than 1% for most measurements, except 7.5% and 5.5% for the measurements of the ^{152}Eu source without and with collimator, respectively. The Genie-2k software automatically corrected dead-time losses because the MCA worked in the live-time mode. Besides, the measurement of environmental background radiations also was carried out.

For the data analysis, the background spectrum was subtracted from the spectra obtained with the radioactive sources. Then, these spectra were processed with the COLEGRAM software that uses the least squares method to fit mathematical functions to experimental data (Lépy, 2004). The full energy peak and escape peak were fitted using a Gaussian function.

The absolute efficiency and relative uncertainty for each full energy peak were determined using the following equations:

$$\varepsilon_{\exp}(E) = \frac{N_P(E)}{A.\, I(E).\, t} \quad (1)$$

$$u_{\exp}(E) = \sqrt{\left(u_{N_P(E)}\right)^2 + (u_A)^2 + \left(u_{I(E)}\right)^2} \quad (2)$$

where: $N_p(E)$ is the net peak area for each energy, A is the source activity (Bq), I(E) is the photon emission intensity, t is the acquisition live time (s). Besides, $u_{N_P(E)}$, u_A, and $u_{I(E)}$ are the relative uncertainty of the net peak area, the source activity, and the photon emission intensity, respectively.

3. Monte Carlo simulations

3.1. Characteristics of Monte Carlo simulation using MCNP6 code

As a new feature in the MCNP6 code, the cutoff energy for the photon transport was set at 1 eV (Goorley et al., 2016). Besides, it also provides a more complete representation of photon scattering and atomic relaxation. The databases of photon interaction and atomic relaxation (from ENDF/B-VI.8 release) are included in the new electron-photon-relaxation data library (eprdata12). Since this library is not the default one, it must be selected by requesting .12p on the material cards (Pelowitz, 2013).

The F8 tally, which is immediately suitable for calculating the detector response, was used to obtain the deposited energy distribution

per incident photon in the crystal volume. In order to achieve compatibility between simulated and experimental spectra, the channels in the simulated spectra were setup based on the energy calibration obtained from the experiments. Besides, the "FT8 GEB a b c" card was used to create the broadening with Gaussian distribution for the peaks in the simulated spectra. The a, b, c coefficients were determined by fitting the experimental data of the full width at half maximum (FWHM) of peaks according to the incident photon energy in the range of 12–60 keV. The FWHM fitting curve was defined by the following equation:

$$FWHM\,(MeV) = a + b \times \sqrt{E + c \times E^2} \quad (3)$$

where: E is the energy of the incident photon (MeV); the values of a, b, c coefficients are 0.000028, 0.001688 and −1.98336 respectively.

The simulated efficiency and relative uncertainty were determined as follows:

$$\varepsilon_{sim}(E) = \frac{N_P(E)}{N(E)} \quad (4)$$

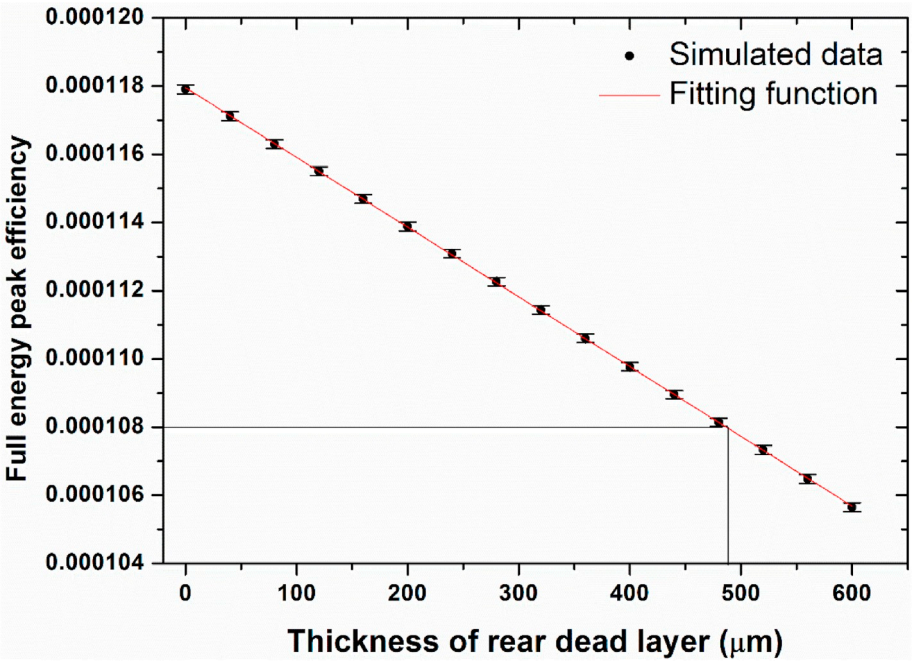

Fig. 6. Fitting with a linear function of simulated efficiency at energy of 59.54 keV for the measurement configuration with collimator according to the thickness of rear dead layer.

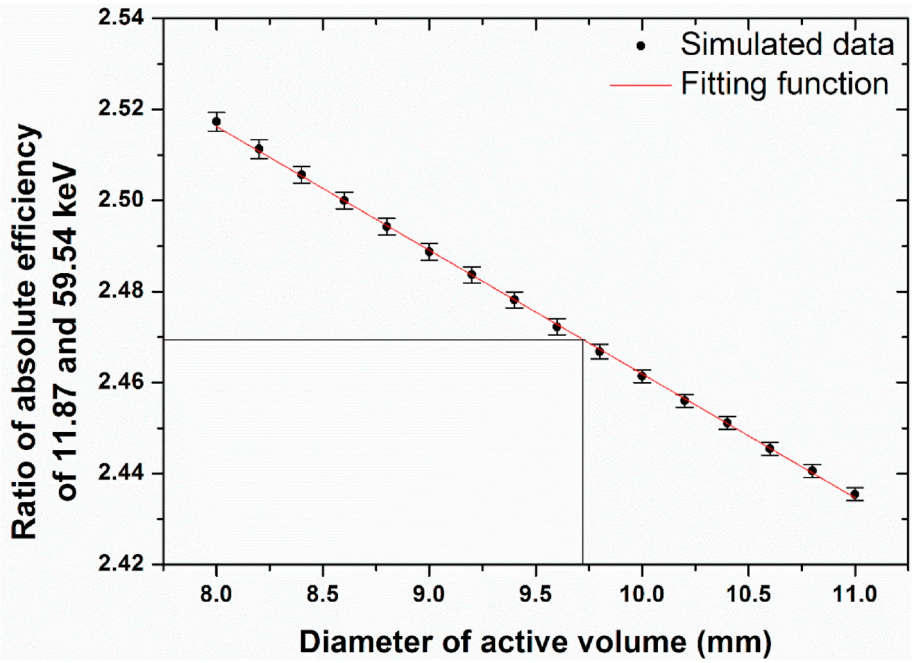

Fig. 7. Fitting with a linear function of the ratio of simulated absolute efficiency of 11.87 and 59.54 keV for the measurement configuration without collimator according to the diameter of active volume.

$$u_{sim}(E) = \frac{\sqrt{N_P(E)}}{N_P(E)} \quad (5)$$

where: $N_P(E)$ is the number of the full energy deposited photons, and N (E) is the number of photons emitted from the source in the MCNP6 simulation.

The number of tracked particles was (3×10^9) and (7×10^9) for the Monte Carlo simulations of measurements without and with collimator, respectively, to keep the relative uncertainty of absolute efficiency less than 0.5%.

3.2. Modeling of Si(Li) detector for Monte Carlo simulations

The schematic representation of the model of Si(Li) detector for Monte Carlo simulations with MCNP6 code is shown in Fig. 1. All components shown are cylindrical in shape. The active volume corresponds to the complete charge collection region of the silicon crystal, the deposited energy of the photon in this volume is fully recorded in the simulated spectra. However, the incomplete charge collection region is not modeled in this work. The inactive volume and dead layers are the regions inside silicon crystal that are not sensitive to radiations, in other words, their charge collection efficiency is zero. Therefore, the deposited energy of the photon in these regions is not recorded in the simulated spectra. The aluminum holder (Mesradi et al., 2008) acts as the inner collimator around the crystal. Its diameter is setup to be equal to the active diameter of silicon crystal.

It is obvious that the components in the real geometry of Si(Li) detectors such as beryllium window, gold contact, front dead layer and possible ice layer (the presence of an ice layer in front of gold contact is suggested by Cohen (1982)) act as absorbing layers and strongly influence the absolute efficiency for low energies. However, the values of most parameters are not given in the manufacturer's specifications. Fernandez et al. (1994) reported different methods for determining the value of these parameters, but the procedures are quite complex. In present study, we propose a simple idea to solve this problem by replacing unknown components by an equivalent layer in the model of Si (Li) detector. Specifically, the thicknesses of the beryllium window and the gold contact are set based on manufacturer's specifications and are kept unchanged during the development of the model of Si(Li) detector. All other absorbing layers are replaced by an equivalent front dead layer that is optimized for the absorption in front of the detector. It is guaranteed that the absorption of incident photons in equivalent layer is equal to the real layers for photon energies higher than 12 keV.

In this study, firstly, an initial model of the Si(Li) detector was constructed based on the manufacturer's specifications. Then, the critical geometric parameters in the model of Si(Li) detector including the thickness of the front dead layer and rear dead layer, the active diameter of crystal, window-crystal distance were improved step-by-step to achieve the optimized model. The values of the geometric parameters and the densities of materials used in initial and optimized models are shown in Table 2. Schematic representation of the configurations with and without collimator for Monte Carlo simulations is shown in Fig. 2. The initial and optimized models of Si(Li) detector were used in Monte Carlo simulations to calculate absolute efficiency for both configurations.

4. Results and discussions

4.1. Evaluation of the initial model

Comparison between simulated efficiency with the initial model of Si(Li) detector and experimental efficiency in the energy range of 12–60 keV for both configurations with and without collimator is presented in Table 3. It is observed that the relative deviations between experimental and simulated efficiencies are in the range of 6–71% and 41–132% for configurations with and without collimator, respectively. Specifically, the simulated efficiency shows a very high discrepancy from experimental efficiency for photon energies below 17.75 keV. Besides, the discrepancy between experimental and simulated efficiencies for the configuration without collimator (average relative deviation of 51%) is higher than the configuration with collimator (average relative deviation of 15%). These results are caused by the difference between the geometric parameters in the initial model and the real geometry of Si(Li) detector. It is obvious that the initial model cannot be used in Monte Carlo simulations to determine the absolute efficiency of Si(Li) detector.

4.2. The optimization of geometric parameters

The four-step procedure is suggested to optimize the critical geometric parameters of Si(Li) detector including the thickness of the front dead layer and rear dead layer, the diameter of active volume, the window-crystal distance. For the optimizations of the thickness of front and rear dead layer, the absolute efficiencies at photon energies of 11.87 and 59.54 keV for the measurement configuration with collimator are used. The diameter of active volume is optimized based on the ratio of absolute efficiencies at photon energies of 11.87 and 59.54 keV for the measurement configuration without collimator. The

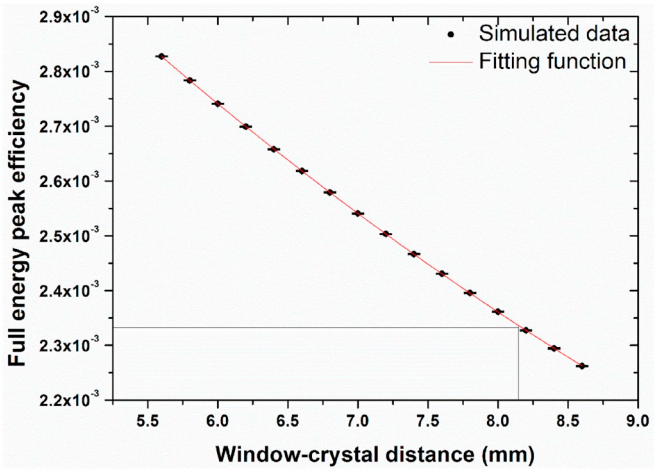

(a)

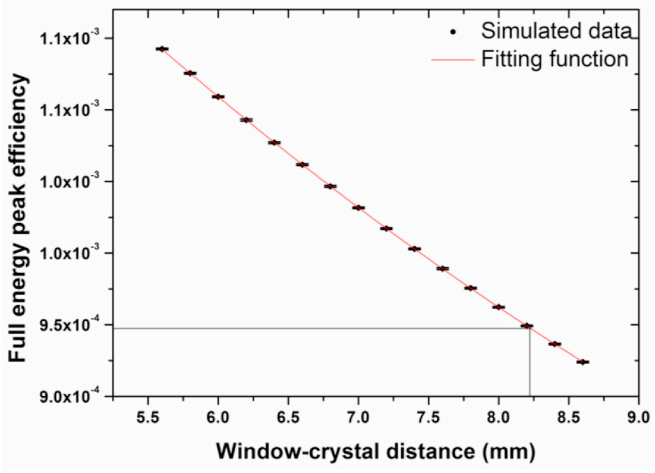

(b)

Fig. 8. Fitting with a quadratic polynomial function of simulated efficiency at photon energies of (a) 11.87 keV and (b) 59.54 keV for the measurement configuration without collimator according to the window-crystal distance.

window-crystal distance is optimized based on the absolute efficiencies at photon energies of 11.87 and 59.54 keV for the measurement configuration without collimator. The simulated data corresponding to various values of interested parameter are fitted by the least squares method with the best suitable mathematical function. Then, the optimized values of the geometric parameters are determined by interpolating the experimental data according to these mathematical functions.

The first optimization is performed for the thickness of the front dead layer. The tracking of the interactions of photons with an energy of 11.87 keV inside the model of Si(Li) detector for measurement configuration with collimator is shown in Fig. 3. It is observed that the interactions of incident photons occur only at locations close to the front surface of silicon crystal, because the energy of photons is not large enough to interact deeply into the crystal. Besides, the width of the interaction area is smaller than the diameter of silicon crystal, because the incident photon beam is collimated. From this result, it can be deduced that the absolute efficiency at energy of 11.87 keV for the measurement with collimator is not affected by the diameter and length of the active volume nor, the window-crystal distance and depends only on the thickness of the front dead layer. Therefore, the experimental efficiency, in this case, is used as reference data to optimize the thickness of the front dead layer in the model of the Si(Li) detector. The decrease of simulated efficiency with an increase in the thickness of the front dead layer according to an exponential function is shown in Fig. 4.

The second optimization is performed for the thickness of the rear dead layer. The sum of the thicknesses of front and rear dead layers and of the length of the active volume is equal to the length of silicon crystal and thus is constant. The increase of the thickness of the rear dead layer causes a decrease in the length of active volume. Therefore, the optimization of the thickness of the rear dead layer is equivalent to the optimization of the length of the active volume. Fig. 5 shows the tracking of the interactions of photons with an energy of 59.54 keV inside the model of Si(Li) detector for the measurement configuration with collimator. It is observed that the interactions of incident photons

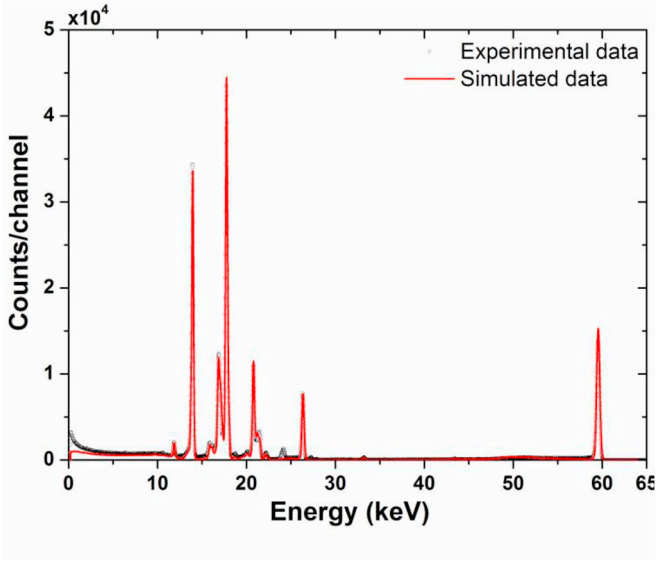

(a)

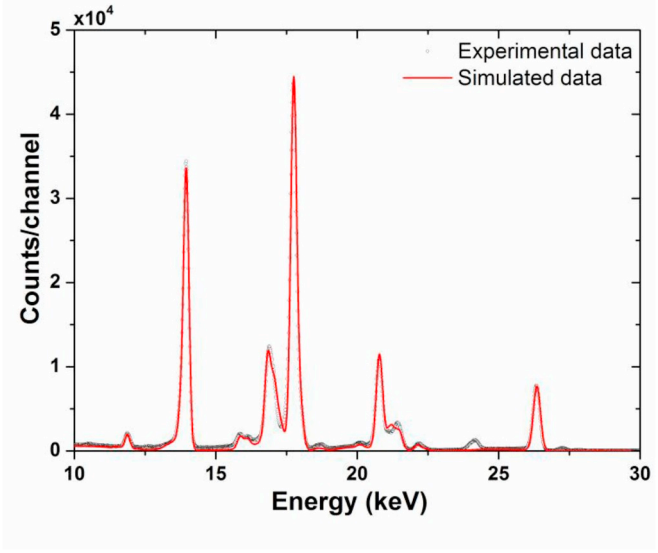

(b)

Fig. 9. Comparison between ^{241}Am simulated spectrum with the optimized model of Si(Li) detector and experimental spectrum for measurement configuration without collimator, (a) full of spectrum and (b) focus on energy below 30 keV.

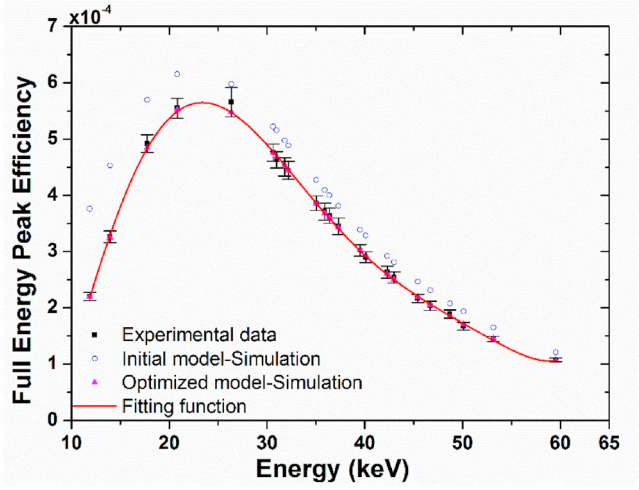

(a)

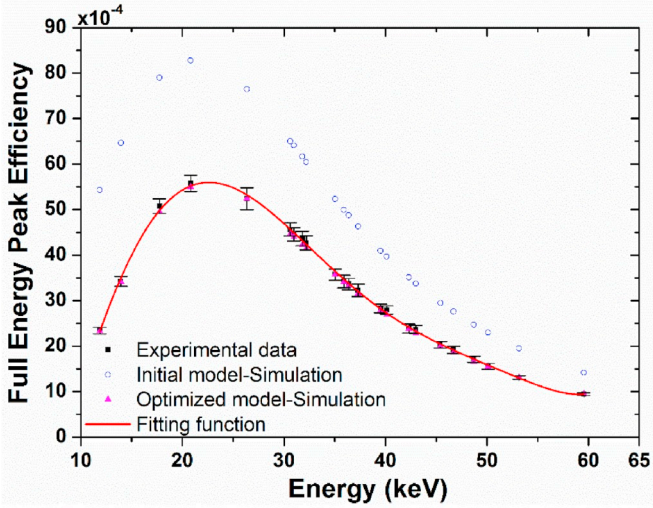

(b)

Fig. 10. Comparison between simulated efficiency with the initial model and optimized model of Si(Li) detector and experimental efficiency for both measurement configurations with (a) and without (b) collimator.

occur at all locations along the length of silicon crystal and the width of the interaction area is smaller than the diameter of silicon crystal. From this result, it can be deduced that the absolute efficiency at energy of 59.54 keV for the measurement with collimator is not affected by the diameter of active volume and the window-crystal distance. Therefore, the absolute efficiency depends only on the length of the active volume or thickness of the rear dead layer. So, this experimental efficiency is used as reference data to optimize the thickness of the rear dead layer in the model of the Si(Li) detector. The decrease of simulated efficiency with an increase in the thickness of the rear dead layer according to a linear function is shown in Fig. 6.

The third optimization is performed for the diameter of the active volume. The absolute efficiency for measurement configuration without collimator is strongly affected by both the diameter of the active volume and the window-crystal distance. Therefore, this quantity cannot be directly used to optimize these parameters because of their self-influence. Our simulated results show that the ratio of the absolute efficiencies at photon energies of 11.87 and 59.54 keV is little affected by the window-crystal distance. Specifically, the values of this ratio only decrease by about 1% when the window-crystal distance increases from 5.6 to 8.6 mm. So, the ratio of the experimental efficiencies at photon energies of 11.87 and 59.54 keV is used as reference data to optimize the diameter of the active volume in the model of the Si(Li) detector. Fitting with a linear function of this ratio according to the diameter of the active volume is shown in Fig. 7.

The last optimization is performed for the window-crystal distance. With the optimizations in the previous steps, the absolute efficiency for measurement configuration without collimator depends only on the window-crystal distance. Therefore, the experimental efficiencies at photon energies of 11.87 and 59.54 keV is used as reference data to optimize this distance. Fitting with a quadratic polynomial function of simulated efficiencies at photon energies of 11.87 and 59.54 keV according to the window-crystal distance is shown in Fig. 8.

Optimized values of the geometric parameters are presented in the second column of Table 2. These values are used to construct an optimized model of Si(Li) detector. In here, the optimization of the front dead layer causes an increase in the absorption of incident photons and a decrease in the active volume of silicon crystal. Therefore, it helps to strongly to reduce the discrepancy between simulated and experimental efficiencies at low energies (below 14 keV). The optimization of the rear dead layer causes a decrease in the active volume at back surface of silicon crystal which it affects the efficiency of incident photons with sufficient energy to transport to the end of silicon crystal. Hence, it helps to reduce the discrepancy between simulated and experimental efficiencies at photon energies above 26 keV. The optimization of the active diameter causes the decrease of the simulated efficiency for all surveyed energies. The optimization of the window-crystal distance helps to decrease the simulated efficiency and its influence is the same for all the energies.

4.3. Verification of the optimized model

Comparison between ^{241}Am simulated spectrum with the optimized model and experimental spectrum is shown in Fig. 9. Besides, a good agreement between simulated efficiency with the optimized model and experimental efficiency in the energy range of 12–60 keV for both configurations with and without collimator is shown in Fig. 10. The comparison between these simulated and experimental efficiencies is presented in Table 4. It is observed that the relative deviations between experimental and simulated efficiencies are less than 4% for all surveyed energies and configurations, and the average relative deviation is about 2%. In most cases, these relative deviations are smaller than the relative uncertainties of the experimental efficiencies. These results demonstrate that the optimized model of the Si(Li) detector is precise and reliable for the use in Monte Carlo simulations to determine absolute efficiency with energies in the range of 12–60 keV.

5. Conclusions

In this study, the simulated efficiency using MCNP6 code with the initial model of Si(Li) detector based on manufacturer's specifications shows a very high discrepancy from experimental efficiency. Therefore, a simple procedure for optimizing the model of Si(Li) detector in the Monte Carlo simulations was presented. The critical geometric parameters of Si(Li) detector including the thickness of the front and rear dead layers, the active diameter of the crystal, the window-crystal

Table 4
Comparison between simulated efficiency with the optimized model of Si(Li) detector and experimental efficiency for both measurement configurations with and without collimator.

E (keV)	With collimator				Without collimator			
	ε_{exp} ($\times 10^{-4}$)	U_{exp} (%)	ε_{sim} ($\times 10^{-4}$)	RD (%)	ε_{exp} ($\times 10^{-4}$)	U_{exp} (%)	ε_{sim} ($\times 10^{-4}$)	RD (%)
11.87	2.20	3.3	2.20	0.1	23.38	3.2	23.29	0.4
13.95	3.26	3.2	3.25	0.3	34.22	3.2	34.10	0.4
17.75	4.92	3.2	4.84	1.6	50.76	3.2	49.48	2.5
20.82	5.55	3.3	5.52	0.5	55.80	3.2	54.98	1.5
26.34	5.65	4.6	5.48	3.1	52.38	4.6	52.41	0.1
30.63	4.76	3.2	4.75	0.1	45.63	3.2	44.61	2.2
30.97	4.63	3.2	4.69	1.3	44.55	3.2	43.96	1.3
31.82	4.51	3.6	4.52	0.3	43.64	3.6	42.24	3.2
32.19	4.44	3.6	4.44	0.1	42.68	3.6	41.42	3.0
35.05	3.86	3.4	3.85	0.1	35.73	3.4	35.71	0.1
35.90	3.71	4.0	3.68	0.7	34.20	4.0	34.06	0.4
36.38	3.64	3.7	3.60	1.1	33.64	3.7	33.23	1.2
37.31	3.45	4.3	3.42	0.8	32.25	4.3	31.55	2.2
39.52	3.02	3.3	3.03	0.3	28.30	3.3	27.82	1.7
40.12	2.90	3.3	2.94	1.4	27.94	3.3	26.93	3.6
42.31	2.63	4.1	2.60	1.1	23.85	4.1	23.78	0.3
43.00	2.54	3.8	2.50	1.6	23.64	3.8	22.82	3.5
45.41	2.17	3.4	2.19	1.0	20.29	3.4	19.91	1.9
46.70	2.04	4.0	2.05	0.7	19.19	4.0	18.61	3.0
48.70	1.89	3.9	1.84	2.8	17.11	3.9	16.61	2.9
50.10	1.67	4.2	1.71	2.3	15.52	4.1	15.46	0.4
53.16	1.45	3.2	1.45	0.3	13.11	3.2	13.10	0.0
59.54	1.08	3.0	1.06	1.6	9.46	3.0	9.50	0.4

distance were optimized based on the interpolation of experimental data according to the fitting functions of simulated data with related variables. The optimized values of these parameters were used to construct an optimized model of the Si(Li) detector for Monte Carlo simulations. This optimized model was validated by comparing the simulated and experimental efficiencies for "point-like" source measurements in two configurations, with and without collimator. The relative deviations between experimental and simulated efficiencies are less than 4% for photon energies in the range of 12–60 keV. This verifies that the proposed procedure is effective to develop the model of Si(Li) detectors in Monte Carlo simulations for different applications. The advantage of this process is simple and easy to implement for most laboratories.

Now, we have a good model of Si(Li) detector for calculating absolute efficiency using MCNP6 code. The next studies will towards setting up a quantitative X-rays fluorescence system in the laboratory. This optimized model of Si(Li) detector will be applied to simulate X-ray fluorescence and scattering (coherent and incoherent) spectra for different samples. The simulated results used to optimize parameters of the system.

Acknowledgment

This research is funded by Vietnam National Foundation for Science and Technology Development (NAFOSTED) under grant number 103.04-2017.303.

Appendix A. Supplementary data

Supplementary data to this article can be found online at https://doi.org/10.1016/j.radphyschem.2019.108459.

References

Campbell, J.L., Leigh, R.G., Teesdale, W.J., 1984. Peripheral imperfections and their effects on efficiency in Si(Li) X-ray detectors. Nucl. Instrum. Methods Phys. Res. B 5, 39–43.

Chechev, V.P., Kuzmenko, N.K., 2010. Decay data evaluation project (DDEP): updated evaluations of the 233Th and 241Am decay characteristics. Appl. Radiat. Isot. 68, 1578–1582.

Cohen, D.D., 1982. M-shell X-ray emission for determining the low energy efficiency of Si (Li) detectors. Nucl. Instrum. Methods Phys. Res. 193 15-10.

Eckert, Ziegler, 2019. Catalogue of reference and calibration sources. https://www.ezag.com/fileadmin/user_upload/isotopes/isotopes/Isotrak/isotrak-pdf/Product_literature/EZIPL/EZIP_catalogue_reference_and_calibration_sources.pdf, Accessed date: 10 April 2019.

Fernandez, L.R., Miranda, J., Oliver, A., 1994. Characterization of a Si(Li) detector for PIXE analysis. J. Xray Sci. Technol. 4, 221–246.

Francis, Z., El Bast, M., El Haddad, R., Mantero, A., Incerti, S., Ivanchenko, V., El Bitar, Z., Champion, C., Bernal, M.A., Roumie, M., 2013. A comparison between Geant4 PIXE simulations and experimental data for standard reference samples. Nucl. Instrum. Methods Phys. Res. B 316, 1–5.

Genie™ 2000 Spectroscopy Software, 2009. Operations. Canberra Industries, Inc.

Goorley, T., James, M., Booth, T., Brown, F., Bull, J., Cox, L.J., Durkee, J., Elson, J., Fensin, M., Forster, R.A., Hendricks, J., Hughes, H.G., Johns, R., Kiedrowski, B., Martz, R., Mashnik, S., McKinney, G., Pelowitz, D., Prael, R., Sweezy, J., Waters, L., Wilcox, T., Zukaitis, T., 2016. Features of MCNP6. Ann. Nucl. Energy 87, 772–783.

Haifa, B.A., Omrane, K., Adel, T., 2007. Si(Li) detector parameters optimization using efficiency calibration. Conference Proceeding of Fundamental and Applied Spectrometry-Ics2007. pp. 223–230.

Incerti, S., Barberet, Ph, Deves, G., Michelet, C., Francis, Z., Ivantchenko, V., Mantero, A., El Bitar, Z., Bernal, M.A., Tran, H.N., Karamitros, M., Seznec, H., 2015. Comparison of experimental proton-induced fluorescence spectra for a selection of thin high-Z samples with Geant4 Monte Carlo simulations. Nucl. Instrum. Methods Phys. Res. B 358, 210–222.

Karamanis, D., 2003. Efficiency simulation of HPGe and Si(Li) detectors in γ- and X-ray spectroscopy. Nucl. Instrum. Methods Phys. Res. 505, 282–285.

Laboratoire National Henri Becquerel, 2019. http://www.nucleide.org/DDEP_WG/DDEPdata.htm, Accessed date: 10 April 2019.

Lépy, M.C., 2004. Presentation of the COLEGRAM Software. Note Technique LNHB 04/26.

Lépy, M.C., Plagnard, J., Ferreux, L., 2008. Measurement of 241Am LX-ray emission probabilities. Appl. Radiat. Isot. 66, 715–721.

López-Pino, N., Padilla-Cabal, F., García-Alvarez, J.A., Vázquez, L., D'Alessandro, K., Correa-Alfonso, C.M., Godoy, W., Maidana, N.L., Vanin, V.R., 2013. Monte Carlo semi-empirical model for Si(Li) X-ray detector: differences between nominal and fitted parameters. AIP Conference Proceeding 1529, 134–136.

Mesradi, M., Elanique, A., Nourreddine, A., Pape, A., Raiser, A., Sellam, A., 2008. Experimental characterization and Monte Carlo simulation of Si(Li) detector efficiency by radioactive sources and PIXE. Appl. Radiat. Isot. 66, 780–785.

Mirion Technologies Inc., 2017. DSA-LX digital signal analyzer. https://www.mirion.com/products/dsa-lx-digital-signal-analyzer, Accessed date: 10 April 2019.

Mirion Technologies Inc., 2017. Silicon Lithium, Si(Li), detectors for X-ray spectroscopy. https://www.mirion.com/products/sili-detector-x-ray-silicon-lithium-detector-for-x-ray-spectroscopy, Accessed date: 10 April 2019.

Pelowitz, D.B. (Ed.), 2013. MCNP6TM User's Manual, Version 1.0. Los Alamos National Laboratory Report LA-CP-13-00634, Rev 0.